



Autologous bone marrow cell implantation attenuates left ventricular remodeling and improves heart function in porcine myocardial infarction: An echocardiographic, six-month angiographic, and molecular–cellular study

Steve Leu^a, Cheuk-Kwan Sun^{b,1}, Jiunn-Jye Sheu^c, Li-Teh Chang^d, Chun-Man Yuen^e, Chia-Hung Yen^f, Chiang-Hua Chiang^g, Sheung-Fat Ko^h, Sung-Nan Peiⁱ, Sarah Chua^a, Ali A. Youssef^j, Chiung-Jen Wu^{a,2}, Hon-Kan Yip^{a,*}

^a Department of Cardiology, Chang Gung Memorial Hospital-Kaohsiung Medical Center, Chang Gung University College of Medicine, Kaohsiung, Taiwan, ROC

^b Department of General Surgery, Chang Gung Memorial Hospital-Kaohsiung Medical Center, Chang Gung University College of Medicine, Kaohsiung, Taiwan, ROC

^c Department of Cardiovascular Surgery, Chang Gung Memorial Hospital-Kaohsiung Medical Center, Chang Gung University College of Medicine, Kaohsiung, Taiwan, ROC

^d Basic Science, Nursing Department, Meiho Institute of Technology, Pingtung, Taiwan, ROC

^e Department of Neurosurgery, Chang Gung Memorial Hospital-Kaohsiung Medical Center, Chang Gung University College of Medicine, Kaohsiung, Taiwan, ROC

^f Department of Life Science, National Pingtung University of Science and Technology, Taiwan, ROC

^g Department of Veterinary Medicine, National Pingtung University of Science and Technology, Taiwan, ROC

^h Department of Radiology, Chang Gung Memorial Hospital-Kaohsiung Medical Center, Chang Gung University College of Medicine, Kaohsiung, Taiwan, ROC

ⁱ Department of Hematology; Center for Translational Research in Biomedical Sciences, Chang Gung Memorial Hospital-Kaohsiung Medical Center, Chang Gung University College of Medicine, Kaohsiung, Taiwan, ROC

^j Department of Cardiology, Suez Canal University Hospital, Ismailia, Egypt

ARTICLE INFO

Article history:

Received 25 September 2009

Accepted 29 March 2010

Available online 13 May 2010

Keywords:

Acute myocardial infarct

Autologous bone marrow-derived stem cell therapy

Molecular–cellular mechanisms

Mini-pigs

ABSTRACT

Background: We investigated the potential benefits and the underlying mechanisms of autologous bone marrow-derived mononuclear cell (BMDMNC) implantation in a porcine model of acute anterior wall myocardial infarction (AAWMI) by studying 6-month left ventricular (LV) function and LV remodeling.

Methods: After being aspirated from the iliac crest and cultured for 1 week, BMDMNCs were implanted immediately after AAWMI induction through the left anterior descending artery ligation. Thirty male mini-pigs (16–18 kg) were equally divided into group 1 [AAWMI plus saline injection into infarct-ischemia area (IA)], group 2 (AAWMI plus 3.0×10^7 BMDMNC transplantation into non-IA), group 3 (AAWMI plus 3.0×10^7 BMDMNC transplantation into IA), group 4 (sham control plus 3.0×10^7 BMDMNC transplantation into LV myocardium), and group 5 (normal control).

Results: By day 90, echocardiography demonstrated an increased LV end-diastolic and end-systolic dimensions but reduced LV ejection fraction (LVEF) in groups 1 and 2 than in other groups (all $p < 0.01$). Six-month angiographic study showed a lower LVEF and wall motion score but a higher mitral regurgitation in groups 1 and 2 than in other groups (all $p < 0.01$). In IA and peri-infarct area, the number of small vessels and mRNA expressions of endothelial nitric oxide synthase, Bcl-2, interleukin (IL)-10, and peroxisome proliferator-activated receptor- γ coactivator-1 α were lower, whereas the number of apoptotic nuclei, caspase-3, Bax, endothelin-1, IL-8, and matrix metalloproteinase was higher in groups 1 and 2 than in other groups (all $p < 0.01$).

Conclusions: Autologous BMDMNC transplantation into IA rather non-IA improves LV function and reduces LV remodeling via eliciting a broad-spectrum of molecular–cellular defensive mechanisms.

© 2010 Elsevier Ireland Ltd. All rights reserved.

1. Introduction

Stem cell therapy has been shown to be a promising strategy for tissue regeneration after injury in various organ systems, including the heart and vascular tissues [1–5]. Although the underlying mechanisms for improving heart function have been proposed to be myogenesis [5], angiogenesis, and vasculogenesis [4,6–8] the exact mechanisms explaining the actions of cytokines [9] on myocardial

* Corresponding author. Division of Cardiology, Department of Internal Medicine, Chang Gung Memorial Hospital, 123, Ta Pei Road, Niao Sung Hsiang, Kaohsiung Hsien, 83301, Taiwan, ROC. Tel.: +886 7 7317123x2363; fax: +886 7 7322402.

E-mail address: han.gung@msa.hinet.net (H.-K. Yip).

¹ The contribution of this author to this work is equal to that of the first author.

² This author contributes equally as the corresponding author to this work.

homing of bone marrow angioblasts [8] and the paracrine effects [7] that attenuate left ventricular (LV) remodeling [9–11] remain poorly defined.

Using small animal models, investigators [4,5,7–9,12] studied the effects of cellular transplantation in various settings of ischemic organ damage and demonstrated consistent findings supporting a therapeutic role of autologous bone marrow-derived mesenchymal stem cells [4,5,9,11]. However, inadequate autologous cells to be implanted for studies on tissue regeneration remain the Achilles' heel when small animals are used. Although allogenic mesenchymal stem cell transplantation has been utilized to tackle this problem [10,13], the issue of immune rejection follows. Additionally, despite the promising results of implanting autologous bone marrow stem cells into the infarct area (IA) following acute myocardial infarction (AMI) [4,5,9,11], the effects of autologous bone marrow stem cells on left ventricular (LV) function when implanted into remote viable myocardium (non-IA) or normal heart without infarction have not been addressed. The limited heart size of small animals further contributes to the difficulty in discriminating between the IA and non-IA for relevant studies.

Anesthetic agents have diverse pharmacological profiles and may exert adverse influences on basal cardiac function that introduce unwanted variables in interpreting data obtained from anesthetized small animals [14,15]. Anatomically, it is well recognized that small animals only have a single left coronary artery as compared with a fully functional differentiation of left coronary artery stem with left main trunk, left anterior descending artery (LAD), and left circumflex artery in human beings. Therefore, the heart size and vascular anatomy of small animals preclude the possibility of clinically relevant coronary angiographic studies. Studies on large animals, on the other hand, can better reflect the clinical condition in an AMI setting.

Beside the anatomical structures of coronary arteries, the mini-pigs also possess many baseline characteristics similar to those of human beings, including the heart rate, ratio of heart to body weight, the arterial and LV blood pressure, as well as LV ejection fraction (LVEF). Of importance is the ease with which coronary angiographic studies and LV angiogram can be performed in the mini-pig. This study, therefore, utilized a mini-pig AMI model through mid-LAD ligation and prompt autologous bone marrow-derived mononuclear

cell (BMDMNC) transplantation to evaluate the potential therapeutic effects using 90-day echocardiographic findings and angiography six months after treatment and to investigate the mechanistic bases of its action on cardiac function and LV remodeling.

2. Methods

2.1. Ethics

All animal experimental procedures were approved by the Institute of Animal Care and Use Committee at our hospital and performed according to the Guide for the Care and Use of Laboratory Animals (NIH publication No. 85-23, National Academy Press, Washington, DC, USA, revised 1996).

2.2. Animals, protocol, procedures

Male mini-pig (Taitung Animal Propagation Station, Livestock Research Institute, Taiwan), weighting 16–18 kg, was anesthetized by intramuscular injections of ketamine (15 mg/kg) and maintained with an inhalation of 1.5% isoflurane during the procedures. After being shaved on the chest, the mini-pig was placed in supine position on a warming pad at 37 °C followed by endotracheal intubation with positive-pressure ventilation (180 ml/min) with room air using a ventilator (Sn: Q422ZO, SIMS PneuPAC, Ltd.). Electrocardiogram (ECG) monitor and defibrillator were then connected to the chest wall. One amp of amiodarone (150 mg) was intravenously given to each animal before the procedure.

Under sterile conditions, the heart was exposed through mid-thoracotomy. After gentle removal of the pericardium, the mid-LAD was doubly ligated with 5-0 prolene suture just after the first diagonal branch. Regional myocardial infarct-ischemia area (IA) is confirmed by observing a rapid whitish discoloration of the anterior wall of LV, followed by a reddish-black discoloration and the development of akinesia as well as dilatation in the at-risk area (defined as IA) (Fig. 1: upper panel). Acute anterior wall myocardial infarction (AAWMI) was confirmed by complete ECG following the procedure (Fig. 1: lower panel).

Mid-LAD ligation was performed in 18 mini-pigs which were equally divided into group 1 [AAWMI plus saline (1000 µl) injection in infarct-ischemia area (IA), $n=6$], group 2 [AAWMI plus BMDMNC implantation into the non-IA (the remote viable LV myocardium)] and group 3 (AAWMI plus BMDMNC implantation into the IA). One-week cultured BMDMNCs (3.0×10^7) in 1000 µl culture medium DMEM were immediately implanted into IA of group 3 and non-IA of group 2 following AAWMI induction (Fig. 1: upper panel). Another 12 mini-pigs were equally divided into group 4 [sham control (thoracotomy without LAD ligation) plus 3.0×10^7 BMDMNC implantation into LV myocardium] and group 5 (normal control). The muscle and skin were then closed in layers. The animals were allowed to remain on the warming pad and recover under care. For identifying BMDMNCs engrafted in the IA, LAD ligation followed by

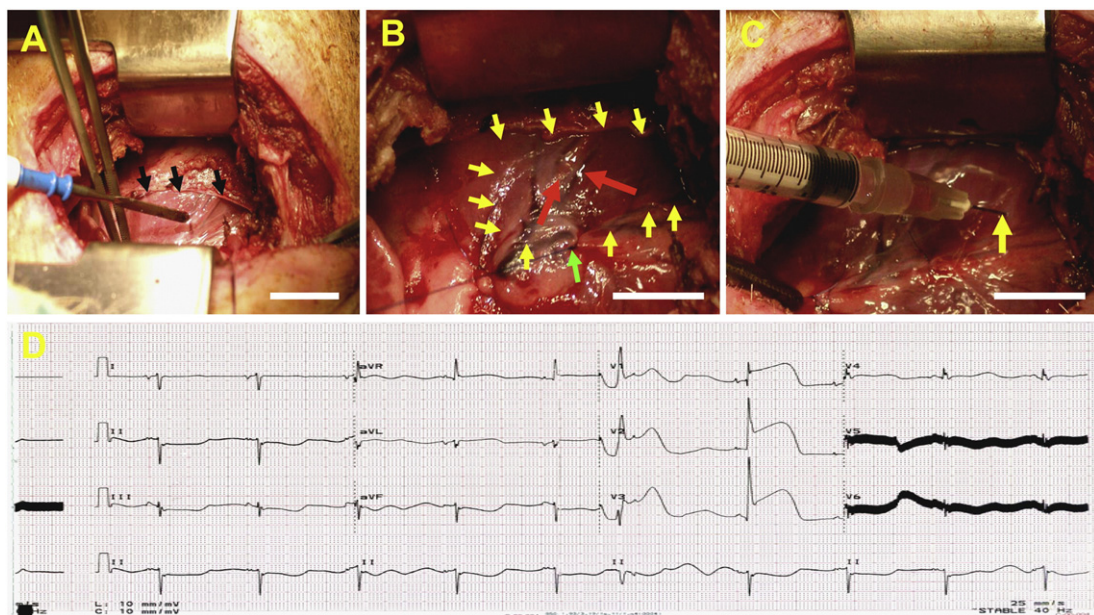


Fig. 1. A) Dissection of pericardium (black arrow) and heart exposure after thoracotomy in a mini-pig. B) Dark-reddish discoloration of ischemic area (yellow arrows) over left ventricular wall (red arrows) after left anterior descending (LAD) ligation (green arrow). C) Implantation of bone marrow-derived mononuclear cells into infarct area. D) Acute ST-segment elevation shown on ECG after LAD ligation. Scale bars represent 15 mm.

BMDMNC implantation were done in other four additional mini-pigs which were sacrificed on day 90 after AMI induction.

2.3. Preparation of BMDMNCs for autologous transplantation

Under general anesthesia, BMDMNCs were aspirated from iliac crest of group 2 and group 3 animals one week before AMI induction. The detailed procedures of separating BMDMNCs after aspiration and cell culture have been recently described [9]. Briefly, BMDMNCs were cultured in DMEM high glucose medium supplemented with 10% bovine serum and antibiotics. Non-adherent hematopoietic cells were removed using this method and the medium was replaced. The BMDMNC (a mixture of weak adherent cells) population contained about 3.0×10^7 cells by one week after they were first plated.

The 5-azacytidine (Sigma) [300 μ l in 3 ml high glucose DMEM (10% FBS)] was added to culture medium on day 3 following BMDMNC culture for 24 h stimulation before implantation. On day 7, 30 min before implanting BMDMNCs, CM-Dil (Vybrant™ Dil cell-labeling solution, Molecular Probes, Inc.) [3 μ l in 3 ml high glucose DMEM (serum free)] was added to the culture medium. This highly lipophilic carbocyanine dye, which has properties of low cytotoxicity and high resistance to intercellular transfer, can be added directly to normal culture media to uniformly label suspended or attached culture cells for their visibility in an implanted area due to its distinctive fluorescence.

2.4. Immunocytochemical staining

The BMDMNCs were also obtained from other six additional mini-pigs. These BMDMNCs (3.0×10^6 cells/pig) were then cultured in 10 ml DMEM culture medium to test for the presence of troponin I positively-stained cells, bone marrow-derived mesenchymal stem cells (CD90 and CD271) and endothelial progenitor cells (CD31 and CD62E) on days 7 and 21, respectively. Then 5-azacytidine was added into the culture medium on day 3 following culturing for 24 h stimulation.

2.5. Functional assessment by echocardiography

Transthoracic echocardiography was performed preoperatively and on day 90 after AMI induction under anesthesia as described previously [16,17] using a commercially available echocardiographic system (UF-750XT) equipped with a 8-MHz linear-array transducer for animals (FUKUDA Denshi Co. Hongo, Bunkyo-Ku, Tokyo, Japan). With the animals in a supine position, left ventricular internal dimensions [i.e. end-systolic diameter (ESD) and end-diastolic diameter (EDD)] were measured according to the American Society of Echocardiography leading-edge method using at least 3 consecutive cardiac cycles [17]. The LV ejection fraction (LVEF) was calculated as: $LVEF = [(LVEDD^3 - LVESD^3) / LVEDD^3] \times 100$. All measurements were performed by an animal cardiologist blind to treatment and non-treatment groups.

(%) = $[(LVEDD^3 - LVESD^3) / LVEDD^3] \times 100$. All measurements were performed by an animal cardiologist blind to treatment and non-treatment groups.

2.6. Cardiac catheterization and definition

By six months following BMDMNC implantation, cardiac catheterization was performed via right common carotid artery. A 6-French pigtail was used for measuring the arterial blood pressure in ascending aorta, LV systolic and end-diastolic pressure and left ventriculography. Coronary angiographic study was performed using a 6-French Kimmy guiding catheter (Boston Scientific, Scimed, Inc. Maple Grove, MN).

Left ventriculography, which was immediately performed after the insertion of arterial sheath into right common carotid artery, was recorded for 30° right anterior oblique and 60° left anterior oblique views. LVEF, LV contractility, and the presence or absence of mitral regurgitation (MR) were determined. The MR was conventionally categorized into grades 1 (mild), 2 (moderate), 3 (moderate–severe), and 4 (severe). Coronary collateral flow grade was determined as previously reported.¹⁴

The mini-pigs were sacrificed by intra-coronary injection of potassium chloride in catheterization room after the procedure. The heart was carefully removed, weighted, and the infarct area collected for measuring the wall thickness at papillary muscle level and for immunohistochemical study.

2.7. Immunohistochemical Study

Engraftment of troponin I-positive and CD31-positive BMDMNCs was assessed by examining the previously implanted regions after immunohistochemical labeling with respective primary antibodies, including anti-troponin I (Abcam) and anti-CD31 (Serotec) as well as secondary anti-mouse conjugate FITC antibodies (Molecular Probe), followed by incubation for 30 min at room temperature. Irrelevant antibodies were used as negative controls.

2.8. Measurement of infarcted wall thickness at papillary muscle level

To determine the impact of BMDMNC therapy on myocardial regeneration, three cross sections of LV at papillary muscle level were observed with three thickest regions chosen and the thickness measured for each animal. The variables were further summed and divided by 6 for statistical analysis for each animal. All measurements were performed by a technician blinded to the treatment and non-treatment groups.

2.9. Real-time quantitative PCR analysis

Real-time polymerase chain reaction (RT-PCR) was conducted using LighCycler TaqMan Master (Roche, Germany) in a single capillary tube according to the

Table 1

Summarized data on body weight, final heart weight, LV dimension, LV function and 6-month angiographic results in 5 groups of mini-pigs.

Variables	Group 1 (n = 6)	Group 2 (n = 6)	Group 3 (n = 6)	Group 4 (n = 6)	Group 5 (n = 6)	p value*
Initial BW (kgm)	17.1 ± 0.9	17.1 ± 0.7	16.9 ± 1.0	16.9 ± 1.0	16.8 ± 1.0	0.364
Final BW (kgm)	20.0 ^a ± 1.7	20.8 ^a ± 1.3	25.1 ^b ± 1.2	26.3 ^b ± 1.4	26.6 ^b ± 1.5	0.0149
Final HW (gm)	133.8 ^a ± 4.5	127.6 ^b ± 6.5	105.8 ^c ± 4.3	99.9 ^c ± 6.0	102.0 ^c ± 3.6	<0.0001
Ratio of HW to BW	6.64 ^a ± 0.86	6.01 ^a ± 0.61	4.23 ^b ± 0.29	3.82 ^b ± 0.35	3.84 ^b ± 0.28	0.0376
Initial LVEF (%)	70.5 ± 7.3	68.7 ± 5.8	71.3 ± 5.6	70.7 ± 4.8	70.3 ± 5.9	0.923
Initial LVEDD (mm)	3.06 ± 0.43	3.32 ± 0.27	2.99 ± 0.23	3.17 ± 0.19	3.07 ± 0.28	0.375
Initial LVESD (mm)	1.87 ± 0.36	2.05 ± 0.11	1.93 ± 0.33	1.94 ± 0.40	1.86 ± 0.19	0.766
90-day LVEF (%)	45.2 ^a ± 4.0	50.0 ^a ± 3.7	58.1 ^b ± 3.6	70.4 ^c ± 5.4	71.4 ^c ± 5.1	<0.0001
90-day LVEDD (mm)	3.68 ^{a,b} ± 0.23	3.78 ^b ± 0.19	3.44 ^a ± 0.29	3.02 ^c ± 0.14	2.93 ^c ± 0.38	<0.0001
90-day LVESD (mm)	2.94 ^a ± 0.23	2.95 ^a ± 0.15	2.43 ^b ± 0.27	1.87 ^c ± 0.11	1.74 ^c ± 0.24	<0.0001
Angiographic results						
Heart rate (beat/min)	99.8 ± 13.9	98.0 ± 22.7	98.2 ± 14.5	94.7 ± 18.4	103.0 ± 8.2	0.957
AsAo SBP (mm Hg)	127.3 ± 25.2	120.8 ± 34.4	130.5 ± 34.4	116.0 ± 12.7	117.2 ± 12.8	0.819
AsAo DBP (mm Hg)	74.3 ± 31.5	77.3 ± 35.2	94.8 ± 34.7	74.5 ± 13.7	76.3 ± 11.8	0.671
LV-SP (mm Hg)	141.2 ± 44.9	151.7 ± 29.5	142.8 ± 29.6	135.8 ± 17.8	126.0 ± 19.6	0.693
LV-EDBP (mm Hg)	19.2 ± 5.9	19.8 ± 9.6	13.7 ± 4.8	10.7 ± 4.1	10.7 ± 5.6	0.0541
LVEF (%)	33.3 ^a ± 9.5	43.8 ^a ± 10.0	58.3 ^b ± 11.0	65.3 ^b ± 10.3	64.0 ^b ± 6.4	<0.0001
Wall motion (%)						
Anterobasal	14.3 ^a ± 5.1	16.0 ^a ± 13.3	27.0 ^b ± 5.7	28.7 ^b ± 9.5	33.0 ^b ± 9.9	0.006
Anterolateral	12.0 ^a ± 8.4	19.5 ^a ± 13	30.2 ^b ± 9.3	35.7 ^b ± 7.8	33.7 ^b ± 10.2	0.003
Apical	12.8 ^a ± 9.1	11.5 ^a ± 1.8	15.0 ^{a,b} ± 8.3	23.0 ^b ± 7.6	18.8 ^{a,b} ± 7.4	0.038
Diaphragmatic	19.0 ± 6.3	16.5 ± 7.8	28.7 ± 12.1	23.5 ± 14.1	29.5 ± 11.2	0.128
Posterobasal	18.0 ^a ± 8.4	17.8 ^a ± 1.7	27.8 ^b ± 6.5	27.7 ^b ± 7.9	23.8 ^b ± 6.6	0.012
Mitral regurgitation	2.17 ^a ± 1.0	2.17 ^a ± 1.3	0.33 ^b ± 0.82	0 ^b ± 0	0 ^b ± 0	<0.0001
Collaterals	0.50 ^a ± 0.55	0.83 ^a ± 0.41	2.83 ^b ± 0.41	0 ^c ± 0	0 ^c ± 0	<0.0001
Wall thickness (mm)	0.69 ^a ± 0.10	0.80 ^b ± 0.10	1.14 ^c ± 0.13	1.38 ^d ± 0.04	1.40 ^d ± 0.05	<0.0001

BW = body weight; HW = heart weight; EDBP = end-diastolic blood pressure; LVEF = left ventricular ejection fraction; LVEDD = left ventricular end-diastolic dimension; LVESD = left ventricular end-systolic dimension; *Indicates by one-way ANOVA. Letters (a, b, c, d) indicate significant difference (at 0.05 level) by Duncan's multiple comparison procedure.

manufacturer's guidelines for individual component concentrations. Forward and reverse primers were each designed based on individual exon of the target gene sequence to avoid amplifying genomic DNA.

During PCR, the probe was hybridized to its complementary single-strand DNA sequence within the PCR target. As amplification occurred, the probe was degraded due to the exonuclease activity of Taq DNA polymerase, thereby separating the quencher from reporter dye during extension. During the entire amplification cycle, light emission increased exponentially. A positive result was determined by identifying the threshold cycle value at which reporter dye emission appeared above background.

2.10. Vessel density in IA and peri-IA

Immunohistochemical staining of blood vessels was performed with α -SMA (1:400) as primary antibody at room temperature for 1 h, followed by washing with PBS thrice. The anti-mouse-HRP conjugated secondary antibody was then added for 10 min, followed by washing with PBS thrice. The 3,3' diaminobenzidine (DAB) (0.7 gm/tablet) (Sigma) was added for 1 min, followed by washing with PBS thrice. Finally, hematoxylin was added for 1 min as a counter-stain for nuclei, followed by washing twice. For quantification, 3 sections of the infarct area were chosen for each rat and 3 randomly selected high-power

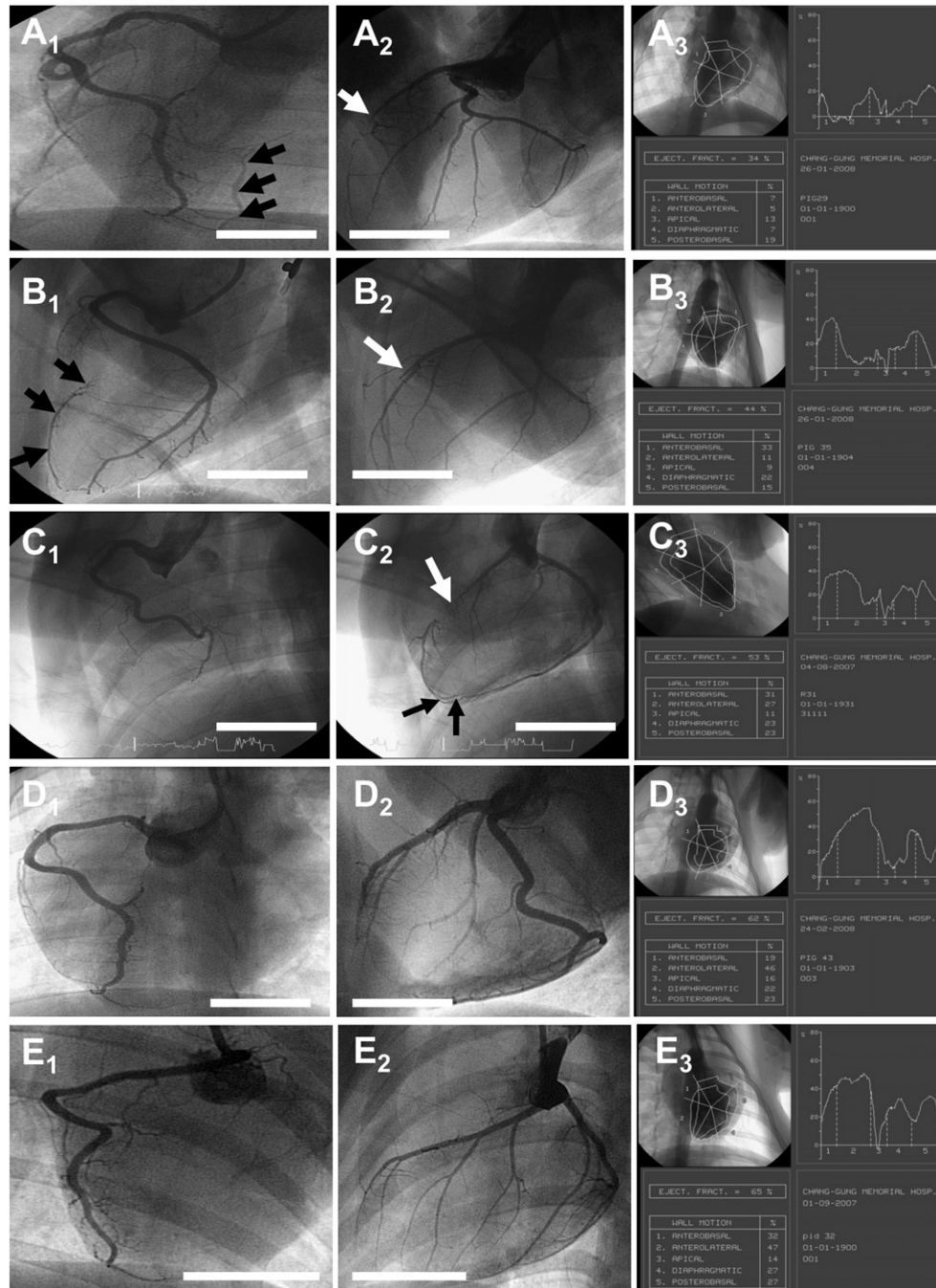


Fig. 2. A₁: Collateral circulation (black arrows) from right coronary artery (RCA) to LAD, A₂: Ligation of middle LAD with intra-coronary collaterals (white arrow), and A₃: Left ventricular (LV) angiogram [LV ejection fraction (EF) = 34%] of AMI-treated by saline only (group 1). B₁: Collateral circulations (black arrows) from RCA to LAD, B₂: Ligation of middle LAD (white arrow) without intra-coronary collaterals, and B₃: LV angiogram (LVEF = 44%) of AMI-treated by bone marrow-derived mononuclear cells (BMDMNCs) implanted into non-infarct area (IA) (group 2). C₁: RCA without collateral from RCA to LAD, C₂: Ligation of middle LAD (white arrow) with intra-coronary collaterals and collaterals form left circumflex artery (black arrows), and C₃: LV angiogram (LVEF = 53%) of AMI-treated by BMDMNCs implanted into IA (group 3). D₁ = right coronary angiography, D₂ = left coronary angiography and D₃ = LV angiogram (LVEF = 62%) of sham control (group 4) treated by BMDMNC implantation into LV myocardium. E₁ = RCA angiography, E₂ = left coronary angiography and E₃ = LV angiogram (LVEF = 63%) of normal control (group 5). Scale bars represent 4 cm.

field (HPF) ($\times 100$) were analyzed for each section. The mean number per HPF for each animal was then determined by summation of all numbers divided by 9.

2.11. TUNEL assay for apoptotic nuclei

For each animal, 6 sections (3 longitudinal and 3 transverse sections of LV myocardium) were analyzed by an in situ Cell Death Detection Kit, AP (Roche) according to the manufacture's guidelines. The TUNEL-positive cells was examined in 3 randomly chosen HPF ($\times 400$) and normalized to the total number of cells divided by 18.

2.12. Statistics analysis

Data were expressed as mean values (mean \pm SD) or (%) of mini-pigs. The significance of differences between groups was evaluated with one-way analysis of variance. Continuous variables among 5 groups were compared using the Duncan's multiple comparison procedure. Data on MR which were not normally distributive were analyzed by Kruskal–Wallis test, followed by multiple comparison procedure with Wilcoxon's rank sum test and Bonferroni's correction. Statistical analysis was performed using SAS statistical software for Windows version 8.2 (SAS institute, Cary, NC). A probability value <0.05 was considered statistically significant.

3. Results

3.1. Initial body weight, final heart and body weight, serial echocardiographic findings and six-month angiographic findings (- Table 1)

Initial body weight did not differ among the five groups. However, the final body weight was significantly lower in groups 1 and 2 than in groups 3, 4, and 5. Conversely, the final heart weight was substantially higher in groups 1 and 2 than in other three groups and significantly higher in group 1 than in group 2. Furthermore, the ratio of final heart to final body weight was notably higher in groups 1 and 2 than in other three groups.

There were no significant differences in initial LVEF, LVEDD, and LVESD among the five groups. Besides, LVEF, LVEDD, and LVESD did not differ between groups 1 and 2 and between groups 4 and 5 on day 90 following BMDMNC implantation. Moreover, LVEDD on day 90

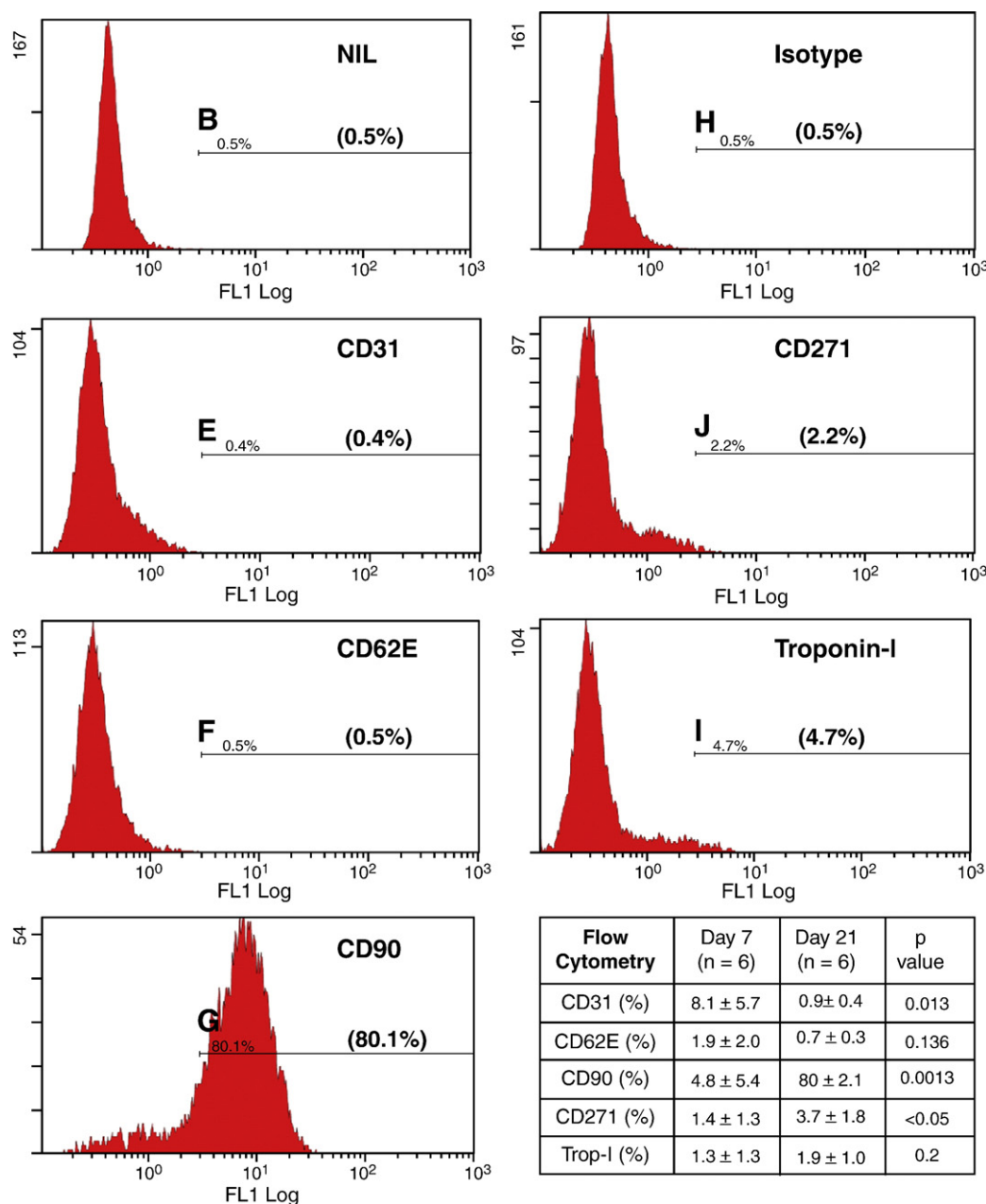


Fig. 3. Flow cytometric histograms on day 21 and the analytic results ($n = 6$) CD31, CD62E, CD90, CD271 and troponin I positively-stained cells on day 7 and day 21 cell culture.

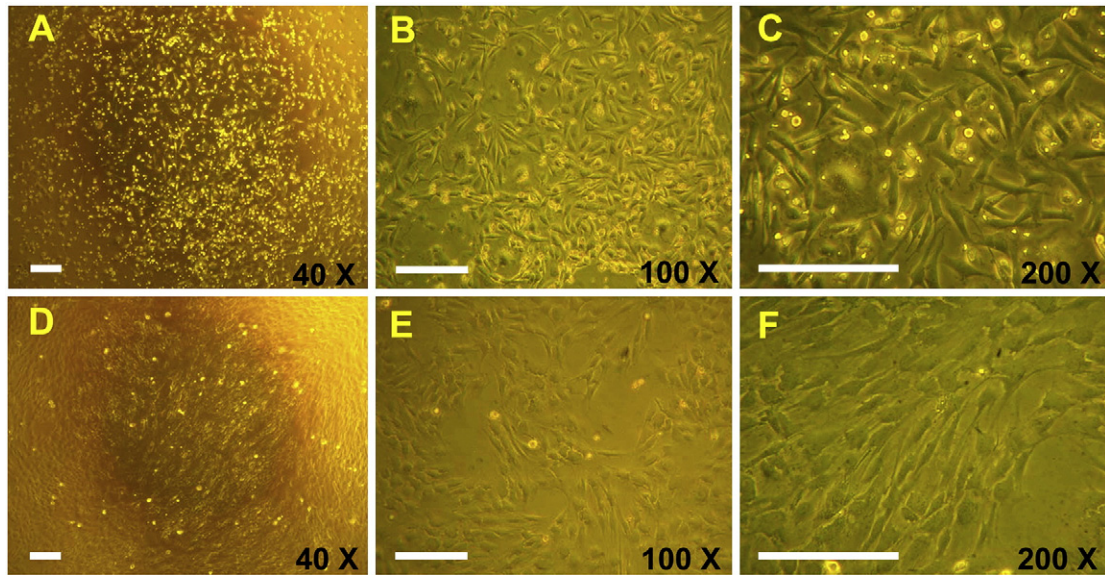


Fig. 4. Following 7 day cell culture, plentiful spindle-shaped BMDMNCs were observed on day 7 (A, B and C). Additionally, cobblestone-like morphology typical for endothelial cells was frequently observed under high-power field of microscope (B and C). However, number of endothelial cells was markedly decreased on day 21 cell culture (E and D). Conversely, more crowded spindle-shaped BMDMNCs with various appearances were observed on culture plate on day 21 cell culture. These findings are comparable with the findings from flow cytometry. Scale bars represent 100 μm .

was similar between groups 1 and 3. However, LVEDD on day 90 was significantly higher in group 2 than in group 3. Furthermore, LVEF on day 90 was substantially lower, whereas LVESD was markedly higher in groups 1 and 2 than in other three groups. In addition, LVEF was significantly lower, whereas LVEDD and LVESD were notably higher in group 3 than in groups 4 and 5 on day 90 following BMDMNC implantation.

Cardiac catheterization was performed on day 180 following BMDMNC implantation. The results demonstrated no significant

differences in heart rate, systolic or diastolic blood pressure of ascending aorta, or LV systolic pressure. However, there was a tendency of higher LVED pressure in groups 1 and 2 than in other three groups ($p = 0.0541$). Additionally, left ventriculogram showed remarkably lower LVEF in groups 1 and 2 than in groups 3, 4 and 5, and a significantly reduced LVEF in group 3 than in groups 4 and 5 (Table 1, Fig. 2). Moreover, the wall motion scores, including anterobasal, anterolateral, and posterobasal, were significantly lower in groups 1 and 2 than in other three groups (Table 1, Fig. 2).

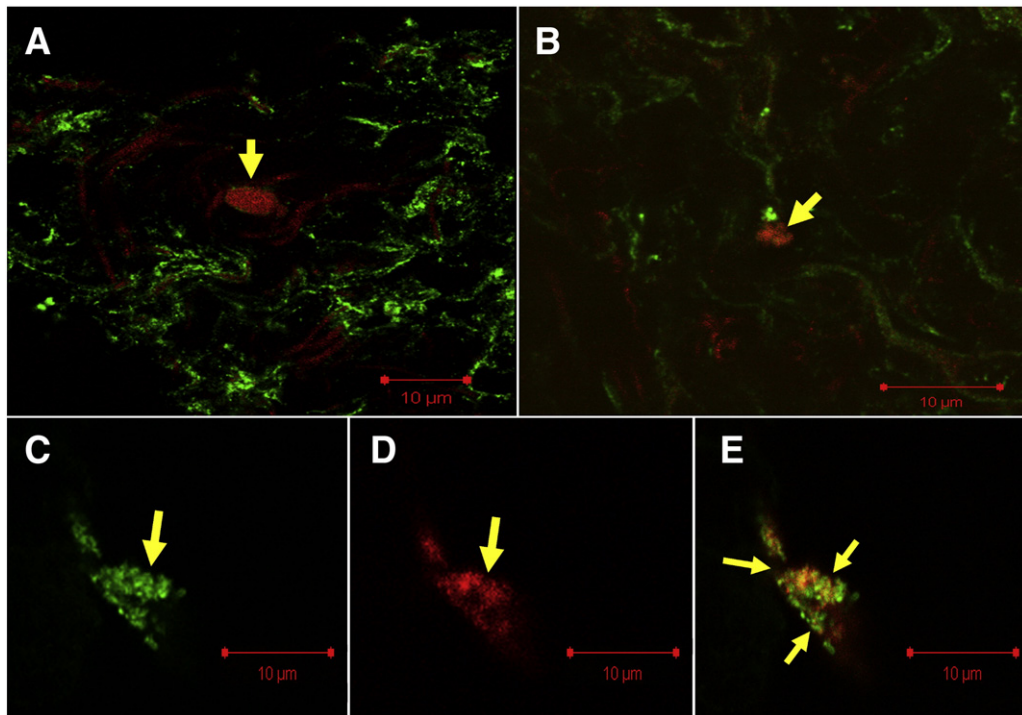


Fig. 5. Confocal image showing CM-Dil positively-stained BMDMNCs (yellow arrow) [A = single cell; B = group of cells] engrafting in troponin I positively-stained LV myocardium in infarct area (IA) by day 90 following AMI induction. Merged image of doubly-stained cells (E) with troponin I (C) and Dil (D) (yellow arrow), showing some implanted BMDMNCs presenting as troponin I-positive myogenic-like cells (green color).

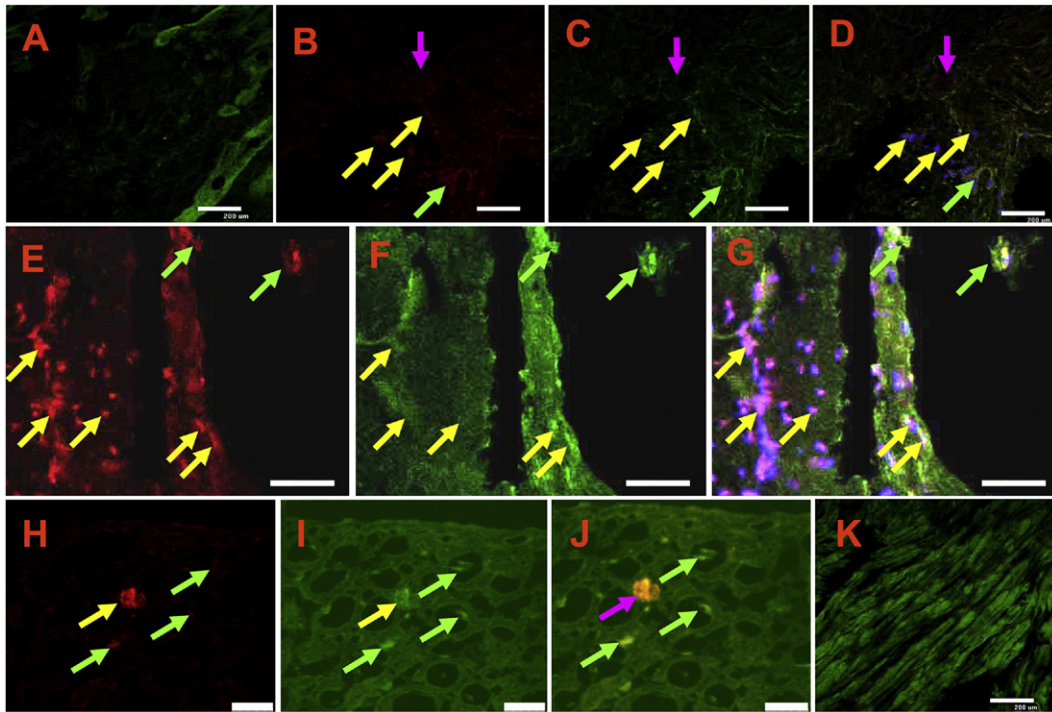


Fig. 6. Confocal imaging study on day 180 following AML induction. Troponin I staining of IA (A) in group 1 with saline-treated only. Merged image (D) of double staining [Dil (B) plus troponin I (C)] (yellow arrows) in group 2 showing some troponin I positive myogenic-like cells (green color) and undifferentiated BMDMBCs (pink arrows) in peri-IA. (D) DAPI staining for nuclei (blue). Merged image (G) of double staining [Dil (E) plus troponin I (F)] (yellow arrows) in group 3 showing only few troponin I-positive myogenic-like cells (green color) and many undifferentiated BMDMBCs (yellow arrows) in IA. Merged image (J) of double staining [Dil (H) plus troponin I (I)] (yellow arrows) in group 4 showing some troponin I-positive myogenic-like cells (green color) and undifferentiated BMDMBCs (pink arrows) in normal myocardium. Troponin I staining of normal myocardium (K) in group 5. Scale bars represent 200 μm in A–D and K, 100 μm in E–G, 25 μm in H–J.

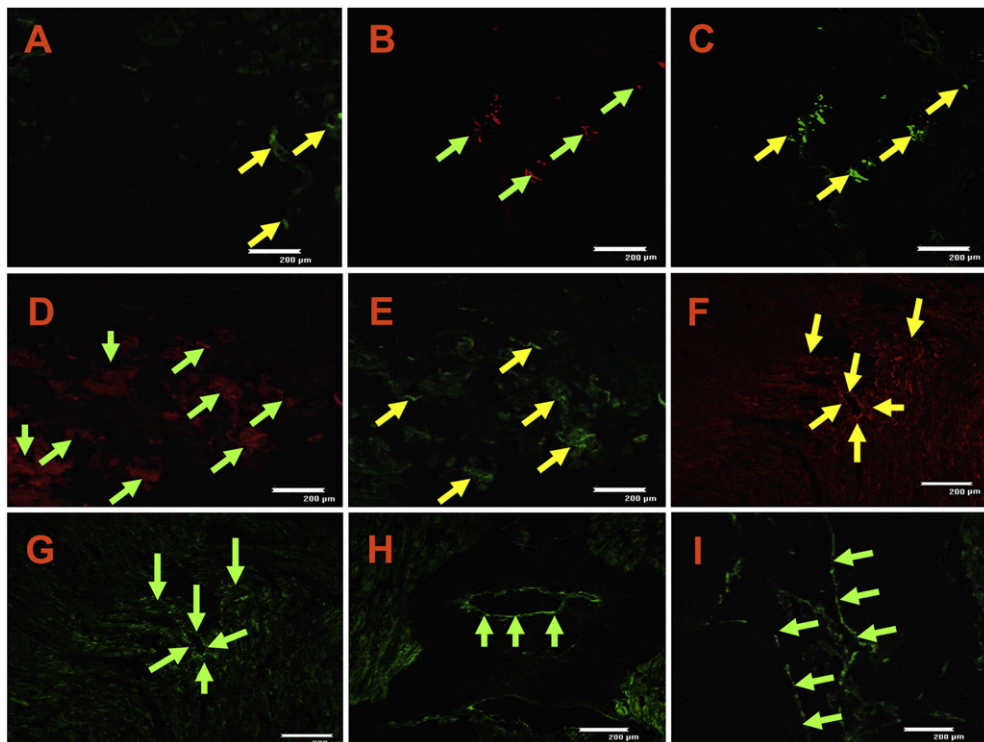


Fig. 7. CD31 positively-stained cells (yellow arrows) indicating endothelial phenotype in peri-IA (A) of group 1. Implanted BMDMNCs in peri-IA of group 2 being doubly-stained with Dil (green arrows) (B) and CD31 (yellow arrow) (C). Double staining of the same cells in IA of group 3 with Dil (green arrows) (D) and CD31 (yellow arrows) (E). Some vessel-like morphology observed in IA (E). Dil positive staining (yellow arrows) (F) and CD31 (green arrows) (G) positive staining in the same cells within normal LV myocardium of group 4. Morphology of a transverse section (F and G) of a small vessel. CD31 positive staining in normal LV myocardium of group 5. Small vessels observed in cross-section (H) and longitudinal section (I). Scale bars represent 200 μm .

The incidence of MR did not differ among groups 3, 4 and 5. However, the incidence of MR was significantly higher in groups 1 and 2 than in other three groups. Furthermore, the collateral circulation was significantly higher in group 3 than in other four groups, and notably higher in groups 1 and 2 than in groups 4 and 5 (Table 1, Fig. 2). Moreover, the wall thickness in IA was significantly lower in group 1 than in other four groups, significantly lower in group 2 than in groups 3 to 5, and notably lower in group 3 than in groups 4 and 5.

3.2. Flow cytometry and microscopic findings of cultured BMDMNCs (Fig. 3)

Wilcoxon's rank sum test of flow cytometric measurements showed that, as compared with day 7 (Fig. 3), the cellular expressions of CD62E and troponin I positively-stained cells did not differ on day 21 following cell culture. However, the cellular expression of CD31 positively-stained cells was markedly decreased on day 21 following cell culture. Conversely, the cellular expressions of bone marrow-derived mesenchymal stem cells (CD90 and CD271) were significantly higher on day 21 following cell culture. These results demonstrated that the population of either endothelial progenitor cells (CD31 and CD62E) or myogenic-like cells (troponin I positively-stained cells) was still relatively low even following a 21-day culturing. In contrast, plentiful spindle-shaped BMDMNCs over the culture plate were found 7 and 21 days following culturing (Fig. 4). These findings indicated a preferential differentiation of BMDMNCs into bone marrow-derived mesenchymal stem cells in the provided culture medium.

3.3. Identification of Implanted BMDMNCs in LV Myocardium (Figs. 5, 6, and 7) by Confocal Imaging Study

By day 90 following BMDMNC implantation, four mini-pigs were sacrificed for identifying differentiated BMDMNCs in LV myocardium. Although numerous CM-Dil-stained undifferentiated BMDMNCs were found to have engrafted, only some CM-Dil-stained engrafted cells presenting as myogenic-like cells (Fig. 5) were stained positively for troponin I.

By day 180 after BMDMNC implantation, the animals in each group were sacrificed with the tissue samples collected for specified studies. Of the CM-Dil-stained engrafted BMDMNCs identifiable using confocal microscopy, some were troponin I-positive and presented as myogenic-like cells (Fig. 6). Additionally, CD31 positively-stained cells, an endothelial phenotype, were also identified in implantation area (Fig. 7).

3.4. Fibrosis of LV myocardium (Fig. 8)

No fibrosis was observed in groups 4 and 5. Moreover, the mean fibrotic area was similar between groups 1 and 2. However, mean fibrotic area in IA was remarkably higher in groups 1 and 2 than in groups 3 on Masson Trichrome staining, whereas it was notably higher in group 3 than in groups 4 and 5 (i.e. negative staining) (Fig. 8).

3.5. RT-PCR and apoptosis

Changes in mRNA expression of interleukin (IL)-8, endothelin (ET)-1, matrix metalloproteinase (MMP)-9, IL-10, endothelial nitric

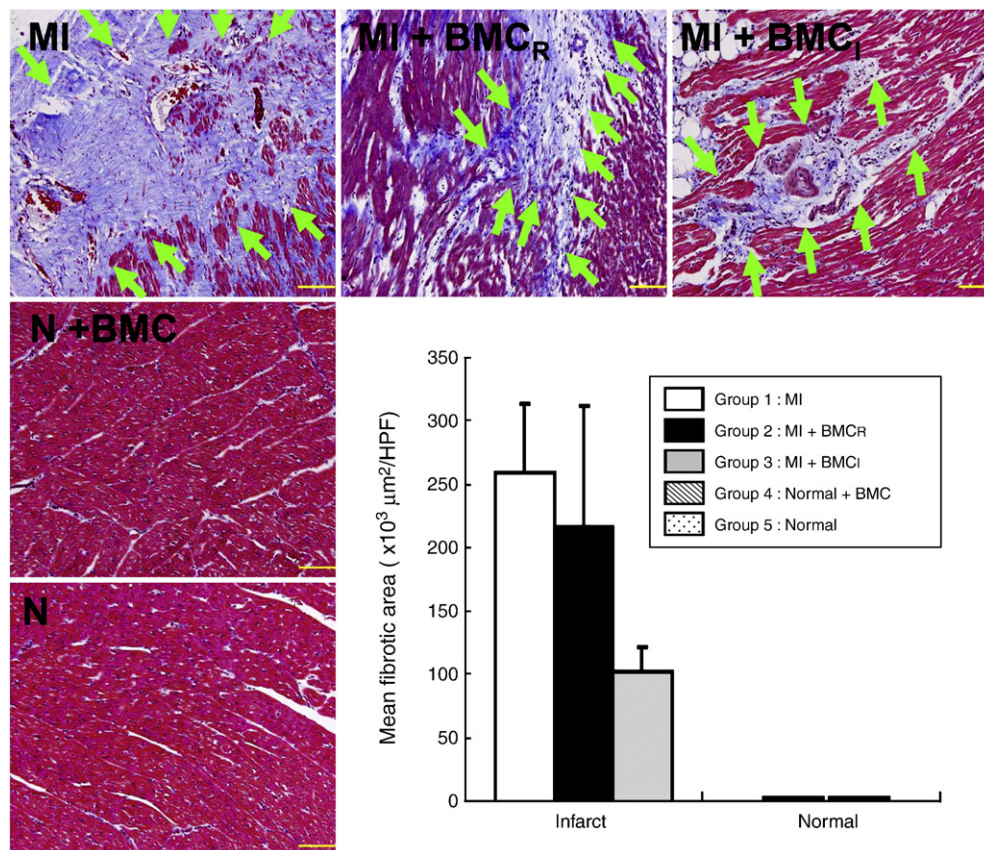


Fig. 8. N = normal; BMC = bone marrow-derived mononuclear cell; MI = myocardial infarction; BMC_R = implantation of BMCs into remote (non-infarct area); BMC_I = implantation of BMCs into infarct area. Mean fibrotic area (μm²/high-power field (HPF) (100×) in each group (n=6) of mini-pigs on day 180 following AMI induction. * vs. †, p = 0.023; * vs. ‡, p = 0.039; † vs. ‡, p = 0.355. Masson's trichrome staining demonstrating markedly reduced fibrosis area (green arrows) in MI + BMC_I group compared to MI only and MI + BMC_R groups. Scale bars in right lower corner represent 50 μm.

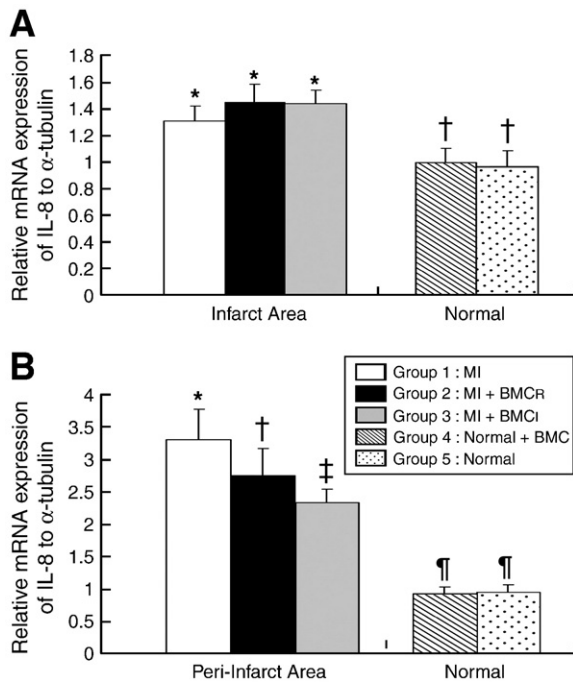


Fig. 9. A) mRNA expression of interleukin (IL)-8 in Infarct area (IA): * vs. †, $p < 0.03$. B) Peri-infarct area (peri-IA): * vs. ‡ or §, $p < 0.05$; † vs. * or ‡, $p > 0.05$; † or ‡ vs. §, $p < 0.0003$.

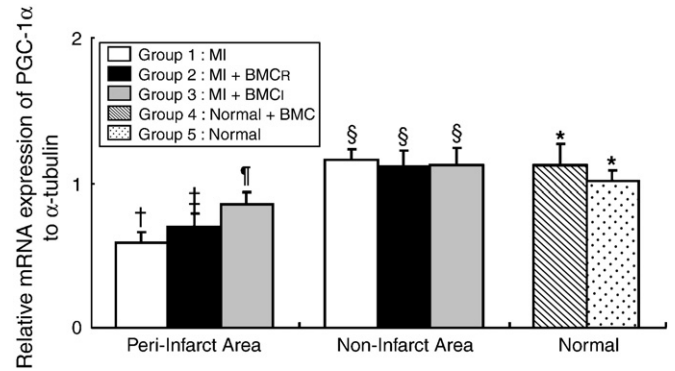


Fig. 11. mRNA expression of peroxisome proliferator-activated receptor- γ coactivator-1 α (PGC-1 α). peri-IA: * vs. † or ‡, $p < 0.002$; § vs. †, $p = 0.024$; § vs. * or ‡, $p > 0.12$; ‡ vs. †, $p = 0.182$. Non-IA: * vs. §, $p > 0.8$.

oxide synthase (eNOS), caspase 3, Bax and Bcl-2 in IA and peri-infarct area (PIA) on day 180 following BMDMNC implantation are shown in Figs. 9, 10 and 11. Moreover, changes of mRNA expression of peroxisome proliferator-activated receptor- γ coactivator-1 α (PGC-1 α) and number of apoptotic nuclei in Peri-IA and non-IA are shown in Figs. 11 and 12D, respectively.

The mRNA expression of IL-8 in IA did not differ in groups 1 to 3. However, it was significantly higher in groups 1, 2 and 3 than in groups 4 and 5. Additionally, it was markedly higher in group 1 than in groups 3, 4 and 5, and significantly higher in groups 2 and 3 than in groups 4 and 5 in PIA.

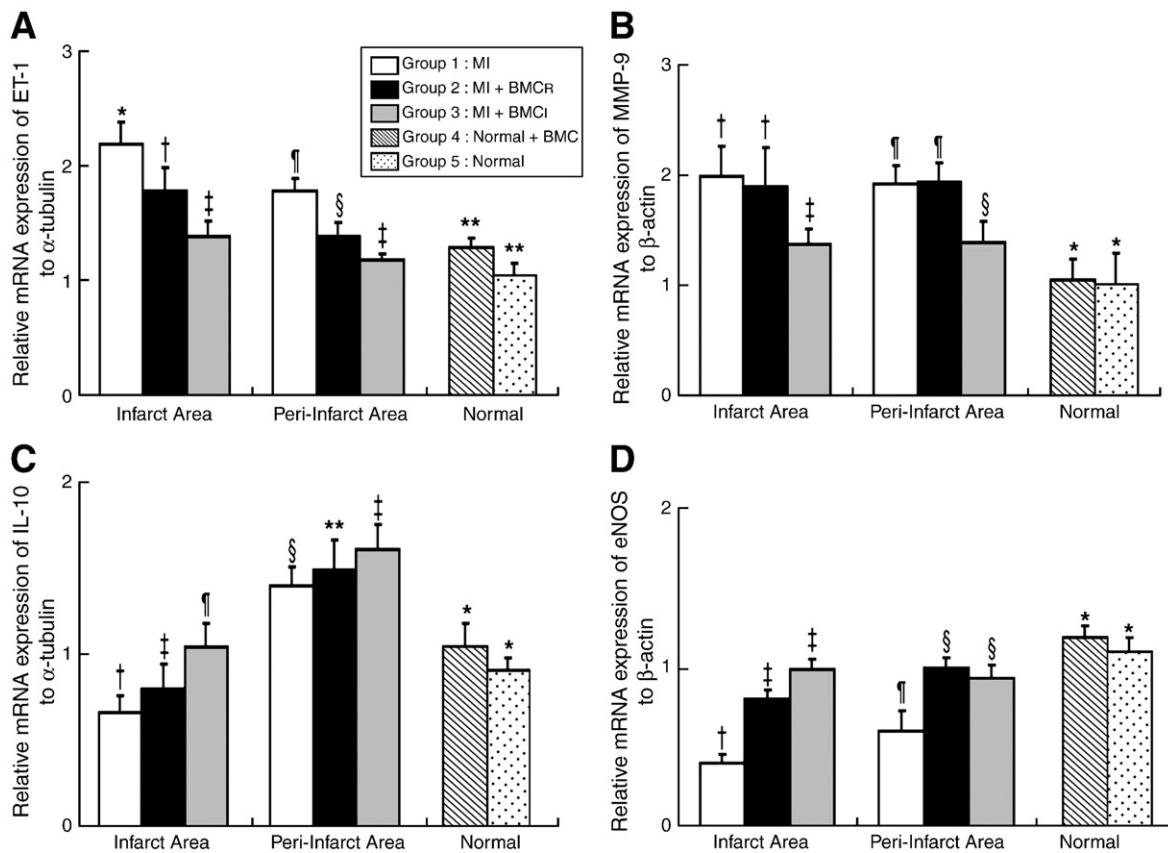


Fig. 10. A) mRNA expression of endothelial-1 (ET-1). IA: * vs. †, ‡ or **, $p < 0.004$; † vs. **, $p < 0.05$; ‡ vs. N, $p = 0.017$; ‡ vs. † or N + BMDMNC, $p > 0.5$. Peri-infarct area (peri-IA): § vs. §, ‡ or **, $p < 0.006$; § vs. **, $p < 0.05$; ‡ vs. **, $p > 0.1$. B) mRNA expression of metalloproteinase 9 (MMP-9). IA: † vs. * or ‡, $p < 0.04$; ‡ vs. *, $p > 0.1$. peri-IA: § vs. § or *, $p < 0.01$; § vs. *, $p > 0.2$. C) mRNA expression of interleukin-10 (IL-10). IA: † vs. * or §, $p < 0.05$; * vs. ‡ or §, $p > 0.3$; ‡ vs. † or §, $p > 0.1$. peri-IA: * vs. §, ‡ or ‡, $p < 0.003$; § vs. ** or ‡, $p > 0.2$; ** vs. ‡, $p > 0.5$. D) mRNA expression of endothelial nitric oxide synthase (eNOS). IA: * vs. †, or MI + BMCR, $p < 0.006$; * vs. IM + BMC, $p > 0.3$; † vs. ‡, $p < 0.006$. peri-IA: § vs. * or §, $p < 0.045$; * vs. §, $p > 0.05$.

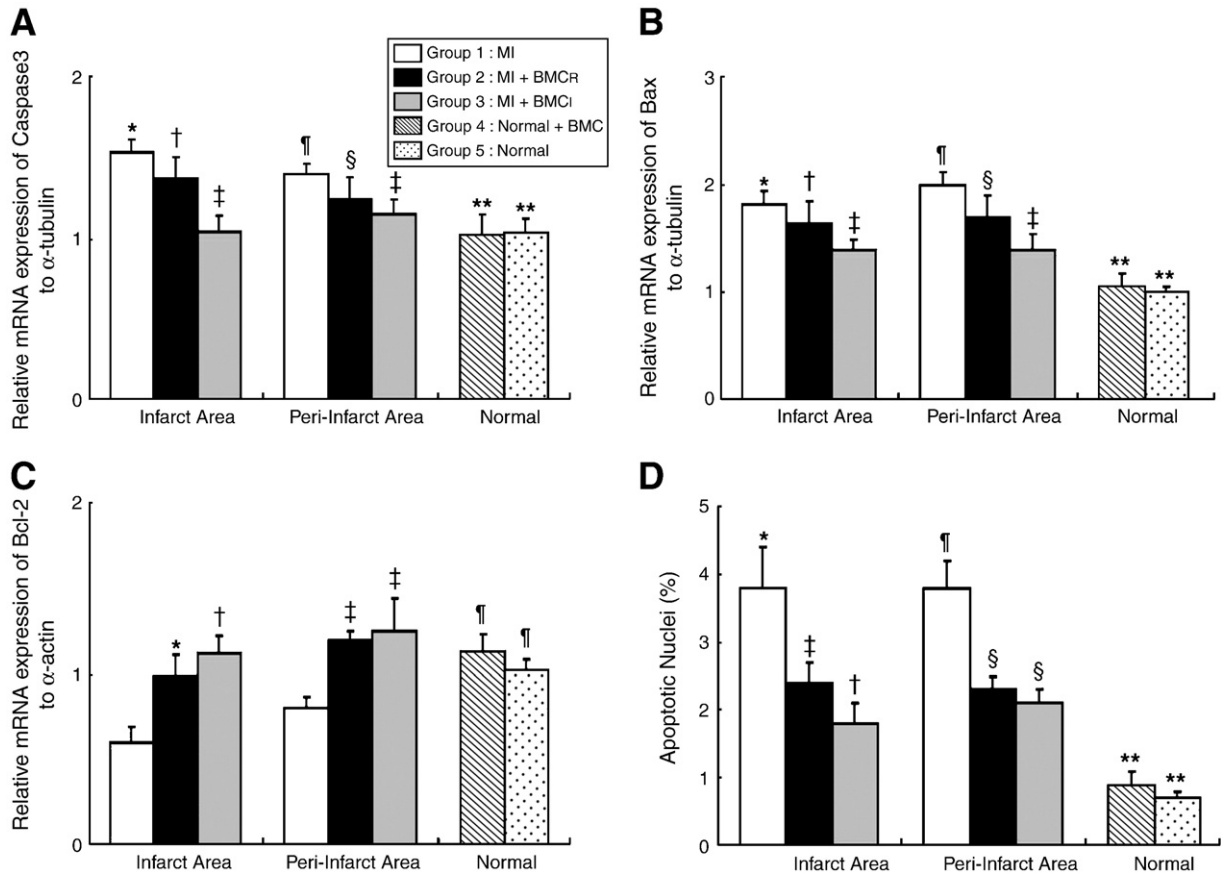


Fig. 12. A) mRNA expression of caspase 3. IA: * vs. ‡ or **, $p < 0.005$; * vs. †, $p = 0.180$; † vs. ‡ or **, $p < 0.05$; ‡ vs. **, $p = 0.439$. peri-IA: § vs. ‡ or **, $p < 0.05$; § vs. †, § or **, $p = 0.103$; ‡ vs. **, $p = 0.2$. B) mRNA expression of Bax. IA: ** vs. *, † or ‡, $p < 0.005$; * vs. ‡, $p = 0.0086$; † vs. * or ‡, $p > 0.05$. peri-IA: ** vs. ‡, § or §, $p < 0.009$; ‡ vs. § or §, $p < 0.05$; § vs. §, $p = 0.07$. C) mRNA expression of Bcl-2. IA: *, † or ‡ vs. MI, $p < 0.05$; § vs. * or †, $p > 0.5$; * vs. †, $p > 0.5$. peri-IA: ‡ or § vs. MI, $p < 0.05$; § vs. ‡, $p > 0.2$. D) Apoptotic nuclei. peri-IA: ** vs. *, † or ‡, $p < 0.004$; * vs. † or ‡, $p < 0.03$; † vs. ‡, $p = 0.145$. Non-IA: § vs. § or **, $p < 0.008$; § vs. **, $p < 0.002$.

The mRNA expression of ET-1 in IA was significantly higher in groups 1 and 2 than in groups 4 and 5, and significantly higher in group 3 than in group 5. Besides, it was notably higher in group 1 than in groups 2 and 3 in IA. Furthermore, its expression in PIA was significantly higher in group 1 than in other groups, and significantly higher in group 2 than in groups 3, 4 and 5. However, the expression in PIA did not differ between groups 3, 4 and 5.

The mRNA expression of MMP-9 in IA and PIA was significantly higher in groups 1 and 2 than in groups 3, 4 and 5. However, it was similar between groups 3, 4 and 5 in IA and PIA.

The mRNA expression of IL-10 in IA did not differ between groups 2 to 5. However, its expression in IA was significantly lower in group 1 than in groups 3, 4 and 5. Additionally, the expression in PIA did not differ between groups 1 to 3, but significantly higher in groups 1 to 3 than in groups 4 and 5.

The mRNA expression of eNOS in IA was significantly lower in group 1 than in other groups, and significantly lower in group 2 than in groups 4 and 5. However, the expression in IA was not different among groups 3, 4 and 5. Although its expression in PIA did not differ between groups 2 to 5, it was significantly lower in group 1 than in groups 2 to 5.

The mRNA expression of caspase 3 in IA did not differ between groups 1 and 2 and among groups 3, 4 and 5. However, the expression in IA was significantly higher in groups 1 and 2 than in groups 3, 4 and 5, but significantly lower in group 1 than in groups 3, 4 and 5 in PIA. Moreover, no difference was noted among groups 2 to 5, and between group 1 and group 2.

No difference was noted in mRNA expression of Bax in IA between groups 1 and 2, groups 2 and 3, or between groups 4 and 5. However, the expression in IA was significantly higher in groups 1, 2, and 3 than in groups 4 and 5, and significantly higher in group 1 than in group 3. Similarly, its expression in PIA was significantly higher in groups 1, 2, and 3 than in groups 4 and 5, and significantly higher in groups 1 and 2 than in group 3. However, its expression in PIA was similar between groups 1 and 2.

The number of apoptotic nuclei in PIA and non-IA was significantly higher in groups 1, 2, and 3 than in groups 4 and 5. However, no significant difference was noted in PIA and non-IA between group 2 and group 3.

The mRNA expression of PGC-1 α in non-IA was similar among the five groups. Moreover, the expression in PIA did not differ among groups 3, 4, and 5, between group 1 and group 2, or between group 2 and group 3. However, it was significantly lower in group 1 than in groups 3 to 5, and significantly lower in group 2 than in groups 4 and 5.

3.6. Small arteriolar density analysis (Fig. 13)

The number of arterioles ($\leq 100 \mu\text{m}$ in diameter) in IA of LV myocardium was substantially higher in groups 2 and 3 than in groups 1, 4, and 5 on day 180 following BMDMNC implantation. Additionally, the number of these small vessels in PIA of LV myocardium was significantly higher in groups 2, 3, and 4 than in

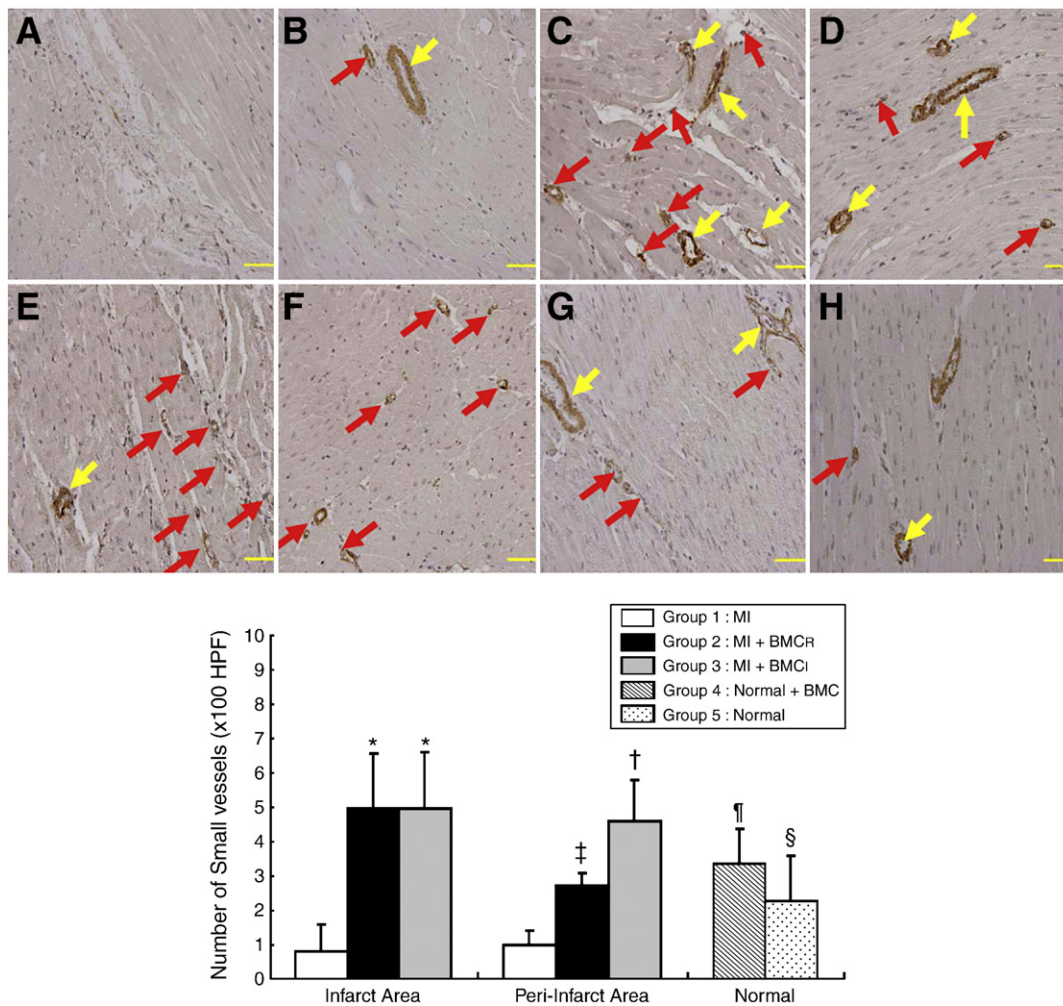


Fig. 13. Identification of small vessel ($\leq 100 \mu\text{m}$) (red arrows) and larger blood vessel ($> 100 \mu\text{m}$) (yellow arrows) distribution using α -SMA immunohistochemical staining (upper panel) on day 180 following BMDMNC implantation. Infarct area (IA) (A) and peri-infarct area (peri-IA) (B) of myocardial infarction (MI) without treatment (group 1). IA (C) and peri-IA (D) of MI plus BMDMNC implanted into non-IA (group 2). IA (E) and peri-IA (F) of MI plus BMDMNC implanted into IA. BMDMNC-implanted area (G) of sham control (group 4) and an area (H) of normal control (group 5). Illustration showing elevated number of small vessel (yellow arrows) in groups 2 and 3 than in other groups in IA, and remarkably increased in group 3 than in other groups in peri-IA ($100\times$). Scale bars in right lower corner represent $50 \mu\text{m}$. η vs. ξ , $p = 0.087$. IA: ξ vs. MI, $p = 0.033$; η vs. MI, $p = 0.004$; * vs. ξ , $p < 0.01$; * vs. η , $p < 0.05$; * vs. MI, $p < 0.001$. Peri-IA: ξ vs. MI, $p = 0.044$; η vs. MI, $p = 0.007$; \dagger vs. ξ , $p = 0.02$; \dagger vs. η , $p > 0.05$; \ddagger vs. MI, $p < 0.008$; \ddagger vs. ξ , $p < 0.01$; \ddagger vs. η , $p > 0.1$; \ddagger vs. ξ , $p > 0.6$.

group 1. These findings indicate that BMDMNC transplantation induced angiogenesis/vasculogenesis mainly in the infarct region in the setting of AMI but to a lesser degree in remote myocardium and negligible effect on normal heart.

4. Discussion

4.1. Impact of BMDMNC transplantation in different scenarios and six-month angiographic findings

There is growing evidence showing improved LV function through autologous BMDMNC transplantation in various settings of ischemic heart diseases [1–8,10,11]. As expected, we found no additional benefit in transplanting autologous BMDMNC into normal heart in enhancing LVEF in this study. Conversely, autologous BMDMNC transplantation into IA markedly improved LVEF and attenuated LV remodeling on day 90 following AMI, and the improvement sustained for 180 days prior to the sacrifice of animals. Interestingly, compared with autologous BMDMNC transplantation into IA, cellular implantation into non-IA was less effective in improving LVEF and reducing LV remodeling in this study. Therefore, these novel findings, in addition to supporting those from

previous studies [1–8,10,11] also highlight the difference in efficacy of BMDMNC transplantation in different regions of the infarcted heart and further refine the underlying therapeutic mechanisms.

4.2. Improvement of LV function and attenuation of LV remodeling following autologous BMDMNC implantation – uncertain mechanisms

Despite the established role of bone marrow-derived stem cell transplantation in improving ischemia-related LV dysfunction [4,5,9–11], the exact mechanism remains unclear [10,18]. Although only a relatively small number of implanted cells were positive for troponin I surface markers on flow cytometric analysis following 21 days of culturing and only a small number of troponin I-positive cells were identified in implanted areas on day 180 after AMI, both echocardiographic and angiographic measurements demonstrated that BMDMNC implantation into IA significantly elevated LVEF, reduced LV chamber size and the incidence of MR in this study compared to animals with AMI treated by saline injection alone. Accordingly, rather than supporting a crucial role of direct cellular participation in limiting LV remodeling and improving LV function, our findings suggest the existence of other unproved confounders.

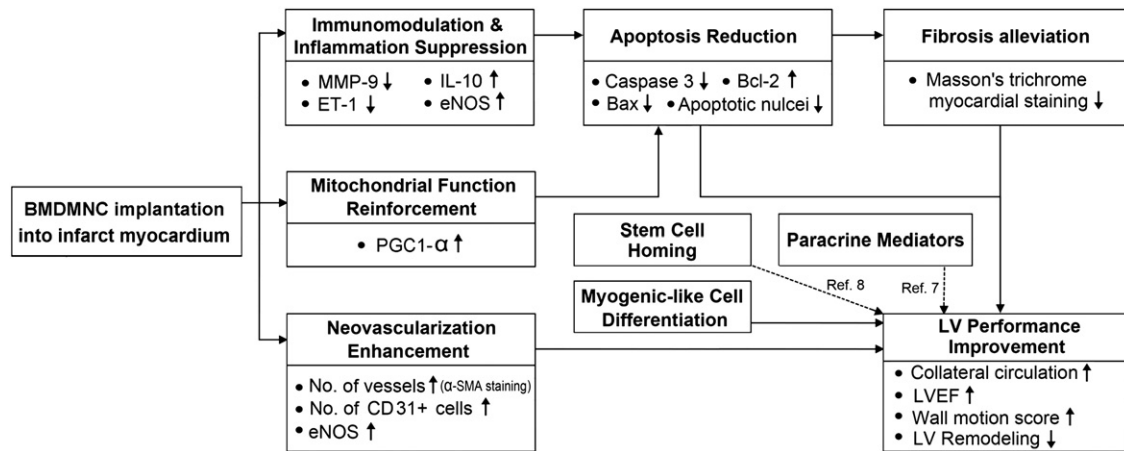


Fig. 14. Schematic presentation of the possible mechanisms of autologous BMDMNC therapy in reducing LV remodeling and improving LV function.

4.3. BMDMNC transplantation modulates immune response and attenuates inflammatory cascades – limiting myocardial damage

There are evidence showing rapid activation of immune responses following AMI, which in turn elicits the complement cascade, inflammatory reaction, reactive oxygen species (ROS) generation, and increased production of inflammatory chemokines [19–24]. This cascade of inflammatory responses causes further myocardial damage following AMI [24]. In the present study, we found that mRNA expressions of MMP-9, IL-8 and ET-1, the three inflammatory chemokines in both IA and peri-IA, were significantly increased in AMI mini-pigs without treatment compared with normal controls. Therefore, our findings are in agreement with those from previous studies [19–24]. Compared with AMI mini-pigs without treatment, these mRNA expressions were markedly suppressed in the BMDMNC IA treatment group. Furthermore, mRNA expressions of the anti-inflammatory cytokine, IL-10, and eNOS, which is an index of nitric oxide (NO) production and enhancer of neovasculation, were markedly upregulated in AMI mini-pigs treated by BMDMNC implantation into IA. These findings implicate that implanted BMDMNCs participate in modulating inflammatory response following AMI. Thum et al. has recently proposed that stem cell therapy modulates immune reactivity by down-regulating innate and adaptive immunity [25]. Our findings support this new perspective concept [25]. Interestingly, the results of the present study showed that, compared with BMDMNC implantation into IA, the anti-inflammatory effects were markedly decreased in cellular implantation into non-IA. The finding highlights the superiority of BMDMNC implantation into IA compared with non-IA for modulating immune response following AMI. Interestingly, a recent study has shown that only early transplanted adequate number of stem cells is able to modulate immune response [26]. Therefore, our suggestion is supported by this recent study [26]. Taken together, we propose three key points for effectively modulating inflammatory reaction following AMI. Firstly, the timing of implantation is preferably immediate after infarct induction. Secondly, adequate BMDMNC population (3.0×10^7) should be used. Thirdly, BMDMNC should be implanted into IA rather than non-IA.

4.4. Contribution of BMDMNC transplantation to angiogenesis/vasculogenesis – enhancing blood and nutrition supply to jeopardized myocardium

Angiogenesis/vasculogenesis has been suggested to play a crucial role in improving ischemia-organ dysfunction [4,6–8]. In this study, in addition to upregulating eNOS mRNA expression, the number of small vessels in both IA and peri-IA was notably increased after BMDMNC implantation. Additionally, CD31 positively-stained cells, an endothelial phenotype, were identified in the BMDMNC-implanted

area. Furthermore, 6-month angiographic results revealed that collateral circulation was markedly increased after BMDMNC implantation into IA. Moreover, the severity of MR, which was at least partly due to ischemic-related papillary dysfunction, was found to be significantly improved after BMDMNC implantation into IA. Therefore, our findings, in addition to strengthening those from previous studies [4,6–9], also explain the reduction in LV remodeling and improvement in LV function on days 90 and 180 after BMDMNC transplantation.

4.5. Wall thickness – results from regeneration and stem cell engraftment into native cardiomyocytes

Previous study has demonstrated that bone marrow cells regenerate in infarcted myocardium [5]. In the present study, although differentiation of BMDMNCs into troponin I-positive cells was uncommon after 21 days of culturing, high population of mesenchymal stem cells were identified by flow cytometry by day 7 and plentiful mesenchymal stem cells in culture plate was observed by day 21 following cell culture. Additionally, although confocal imaging study only identified few Dil-stained myogenic-like cells in IA, many undifferentiated Dil-stained BMDMNCs were found to have engrafted. These findings may, at least in part, explain the significant increase in wall thickness in IA, an index of regeneration, after BMDMNC implantation. Consistent with a previous study [5], this finding could at least partially explain the attenuation in LV remodeling in AMI mini-pig treated by BMDMNC implantation into IA.

4.6. BMDMNC transplantation attenuates cellular apoptosis, myocardial fibrosis and preserves energy transcription pathway – insight into abrogating cardiomyocyte death

Various situations, including CHF, ischemia, dilated LV remodeling or inflammation, may contribute to energy exhaustion and apoptosis of cardiomyocytes [4,9,27–30]. The current study demonstrated that the mRNA expressions of Bax and caspase 3, two indexes of apoptosis, were markedly suppressed and mRNA expression of Bcl-2, an index of anti-apoptosis, was notably enhanced in both IA and PIA on day 180 following BMDMNC implantation into IA. Additionally, this strategic management notably attenuated cellular apoptosis in both PIA and non-IA. Therefore, our results not only strengthen the previous findings [4,9,27–30], but also provide insight into the mechanisms underlying reduction in fibrosis of LV myocardium in AMI after BMDMNC treatment that leads to a significant preservation in cardiac function in the present study.

4.7. Limitations of study

This study has limitation. Although the results of the present study are attractive and promising, the exact mechanisms involved in the improvement of LV function after BMDMNC implantation in AMI mini-pig remain certain. Summarizing the results of the current study, the possible mechanisms of autologous BMDMNC therapy in reducing LV remodeling and improving LV function are schematically presented in Fig. 14.

4.8. Conclusions

The results of this study demonstrate that autologous BMDMNC transplantation is effective in preserving heart function and reducing LV remodeling through eliciting serial molecular–biological defensive mechanisms. Three key points for successful outcomes can be obtained from this study, including prompt cellular implantation after infarct induction, the use of adequate BMDMNC population, and cellular implantation into IA rather than non-IA.

Acknowledgement

This study is supported by a program grant from the National Science Council, Taiwan, ROC (grant no. NSC-96-2314-B-182A-135). The authors of this manuscript have certified that they comply with the Principles of Ethical Publishing in the International Journal of Cardiology [31].

References

- [1] Blau HM, Brazelton TR, Weimann JM. The evolving concept of a stem cell: entity or function? *Cell* 2001;105:829–41.
- [2] Yang S, Fazel S, Angoulvant D, Weisel RD, Li RK. Cell transplantation for heart disease: the clinical perspective. *Evid Based Cardiovasc Med* 2005;9:2–7.
- [3] Nanjundappa A, Raza JA, Dieter RS, Mandapaka S, Cascio WE. Cell transplantation for treatment of left-ventricular dysfunction due to ischemic heart failure: from bench to bedside. *Expert Rev Cardiovasc Ther* 2007;5:125–31.
- [4] Yip HK, Chang LT, Wu CJ, et al. Autologous bone marrow-derived mesenchymal stem cell therapy prevents the damage of viable myocardium and improves rat heart function following acute anterior myocardial infarction. *Circ J* 2008;72:1336–45.
- [5] Orlic D, Kajstura T, Chimenti S, Bodine BM, Leri A, Anversa P. Bone marrow cells regenerate infarcted myocardium. *Nature* 2001;401:701–5.
- [6] Tse HF, Kwong YL, Chan JK, Lo G, Ho CL, Lau CP. Angiogenesis in ischemic myocardium by intramyocardial autologous bone marrow mononuclear cell implantation. *Lancet* 2003;4:47–9.
- [7] Davani S, Marandin A, Merisin N, Royer B, Kantelip B, Herve P. Mesenchymal progenitor cells differentiate into an endothelial phenotype, enhance vascular density, and improve heart function in a rat cellular cardiomyoplasty model. *Circulation* 2003;108:253–8 suppl II.
- [8] Kocher AA, Schuster MD, Bonaros N, Lietz K, Xiang G, Martens TP. Myocardial homing and neovascularization by human bone marrow angioblasts is regulated by IL-8/Gro CXC chemokines. *J Mol Cell Cardiol* 2006;40:455–64.
- [9] Sun CK, Chang LT, Sheu JJ, et al. Bone marrow-derived mononuclear cell therapy alleviates left ventricular remodeling and improves heart function in rat-dilated cardiomyopathy. *Crit Care Med* 2009;37:1487–9.
- [10] Dai W, Hale SL, Martin BJ. Allogeneic mesenchymal stem cell transplantation in postinfarcted rat myocardium: short- and long-term effects. *Circulation* 2005;112:214–23.
- [11] Tang Y, Zhao Q, Qin X. Paracrine action enhances the effects of autologous mesenchymal stem cell transplantation on vascular regeneration in rat model of myocardial infarction. *Ann Thorac Surg* 2005;80:229–37.
- [12] Mazzinghi B, Ronconi E, Lazzeri E, et al. Essential but differential role for CXCR4 and CXCR7 in the therapeutic homing of human renal progenitor cells. *JEM* 2008;205:479–90.
- [13] Forte A, Finicelli M, Mattia M. Mesenchymal stem cells effectively reduce surgically induced stenosis in rat carotids. *J Cell Physiol* 2008;217:789–99.
- [14] Yang XP, Liu YH, Rhaleb NE, Kurihara N, Kim HE, Carretero OA. Echocardiographic assessment of cardiac function in conscious and anesthetized mice. *Am J Physiol (Heart Circ Physiol)* 1999;277:H1967–74.
- [15] Roth DM, Swaney JS, Dalton ND, Gilpin EA, Ross J. Impact of anesthesia on cardiac function during echocardiography in mice. *Am J Physiol (Heart Circ Physiol)* 2002;282:H2134–40.
- [16] Litwin SE, Katz SE, Morgan JP, Douglas PS. Serial echocardiographic assessment of left ventricular geometry and function after large myocardial infarction in the rat. *Circulation* 1994;89:345–54.
- [17] Jiang Y, Jahagirdar BN, Reinhardt RL, Schwartz RE, Keene CD, Ortiz-Gonzalez XR. Recommendations of regarding quantification in M-mode echocardiography: results of a survey of echocardiographic measurements. *Circulation* 1978;58:1072–83.
- [18] Makino S, Fukuda K, Miyoshi S, Konishi F, Kodama H, Pan J. Cardiomyocytes can be generated from marrow stromal cell in vitro. *J Clin Invest* 1999;103:697–705.
- [19] Frangogiannis NG, Smith CW, Entman ML. The inflammatory response in myocardial infarction. *Cardiovasc Res* 2002;53:31–47.
- [20] Lambert JM, Lopez EF, Lindsey ML. Macrophage roles following myocardial infarction. *Int J Cardiol* 2008;130:147–58.
- [21] Frangogiannis NG. The immune system and cardiac repair. *Pharmacol Res* 2008;58:88–111.
- [22] De Scheerder I, Vanderkerckhove J, Robbrecht J, Algoed L, de Buyzere M, de Langhe J. Post cardiac injury syndrome and an increased humoral immune response against the major contractile proteins (actin and myosin). *Am J Cardiol* 1985;56:631–3.
- [23] Lange LG, Schreiner GF. Immune mechanisms of cardiac disease. *New Engl J Med* 1994;330:1129–35.
- [24] Bloom NV, Leor J, Ohad DG, Hasin Y, Amar M, Fixler R. Cytotoxic T lymphocytes are activated following myocardial infarction and can recognize and kill healthy myocytes in vitro. *J Mol Cell Cardiol* 2000;32:2141–9.
- [25] Thum T, Bauersachs J, Poole-Wilson PA. The dying stem cell hypothesis: immune modulation as a novel mechanism for progenitor cell therapy in cardiac muscle. *J Am Coll Cardiol* 2005;46:1799–802.
- [26] Blanc KL, Tammik L, Sundberg B. Mesenchymal stem cells inhibit and stimulate mixed lymphocyte cultures and mitogenic responses independently of the major histocompatibility complex. *Scand J Immunol* 2003;57:11–20.
- [27] Singal PK, Khaper N, Palace V. The role of oxidative stress in the genesis of heart disease. *Cardiovasc Res* 1998;40:426–32.
- [28] Ichihara S, Yamada Y, Ichihara G. Attenuation of oxidative stress and cardiac dysfunction by bisoprolol in an animal model of dilated cardiomyopathy. *Biochem Biophys Res Commun* 2006;350:105–13.
- [29] Garnier A, Fortin D, Delomenie C. Depressed mitochondrial transcription factors and oxidative capacity in rat failing cardiac and skeletal muscles. *J Physiol* 2003;551:491–501.
- [30] Huss JM, Kelly DP. Mitochondrial energy metabolism in heart failure: a question of balance. *J Clin Invest* 2005;115:547–55.
- [31] Coats AJ. Ethical authorship and publishing. *Int J Cardiol* 2009;131:149–50.